

Stress corrosion behaviour of Al–Zn–Mg alloys based upon microchemical surface reactions

ÁGNES CSANÁDY

Research, Engineering and Prime Contracting Centre of the Hungarian Aluminium Corporation, Budapest, Hungary

DÉNES MARTON

Institute for Physics of the Technical University, Budapest, Hungary

Divergences between the chemical compositions of the natural oxide layers on pure aluminium and of alloys containing magnesium have been shown with the aid of SIMS measurements. Scanning and transmission electron micrographs and electron microprobe measurements indicate the sensitizing effect of the thermal oxide layer to water vapour and this is substantiated by SIMS studies.

From published data and this investigation a further elaboration of the possible explanation for stress corrosion is proposed.

1. Introduction

The mechanism of the stress corrosion of Al–Zn–Mg alloys has been a subject of considerable discussion and investigation over the last twenty years or more. A number of theories have been proposed but at present no mechanism is universally accepted. Recently, however, the hydrogen mechanism seems to have been growing in importance [1–3].

Technical literature regards the following microstructural factors as important for explaining stress corrosion fracture:

- (a) the critical dimensions, morphology and distribution of precipitates inside the grain or on the grain boundaries [4];
- (b) the distribution of alloying elements along the grain boundary [5, 6];
- (c) the variation in width of the PFZ (precipitate free zone) [7].

According to pertinent literature stress corrosion is connected with the following phenomena:

- (a) the repeated formation and disruption of oxide films along the PFZ [8];
- (b) the increased movement of dislocations in the PFZ along the grain boundary [9];
- (c) the increased dissolution of areas along the grain boundary [10];

(d) some sort of hydrogen embrittlement [1–3].

It is obvious that the observed microstructural factors and the related phenomena are connected. By our investigations of the oxide layers we try to link some results of microstructural measurements with phenomena characteristic of stress corrosion.

According to Ward and Lorimer [5] the Zn content is lower in the precipitate-free zones (PFZ) or remains at the level of the grain interior. At temperatures where during heat treatment a Zn “profile”, i.e. a lower Zn content appears at the grain boundary or in its vicinity the stress corrosion sensitivity of the alloy Al–6% Zn–3% Mg decreases.

Doig *et al.* [6] have measured the magnesium distribution in the PFZ of the alloy Al–6% Zn–3% Mg. As shown by the magnesium profiles, the various heat treatments resulted in an increase of the magnesium content in the PFZ as compared with the central part of the grains.

The above changes of alloying element concentration of the metal may influence the rate of crack formation or propagation because they can change either the metal solution from the grain boundary zone [10] or the composition and stability of the oxide film or both. The verification of

the change in the composition and stability of the oxide film may be very important as these films are the barriers in the interaction between the alloy and the environment. As recent evidence seems to indicate that hydrogen embrittlement is one, perhaps the dominant, mechanism in stress corrosion cracking [1–3], the investigations of Tuck and Scamans [11] are of great interest. They found that hydrogen penetration in alloy Al–4.3% Zn–1.5% Mg always occurs along the grain boundaries if the samples are stored at 70° C in moist air.

2. Experimental part and interpretation of the results

2.1. Investigations of natural oxide layers

In our investigations we started from the assumption that the alloying element content of the alloy influences the composition of the oxide layer formed on it or rather from it and therefore also the structure of the layer in its more extended sense. If this can be proved on the “macro” scale then our conclusions can be applied also to the effects of inhomogeneous composition and stability of the oxide layer which are due to the micro-inhomogeneity of the alloying elements. Since it is assumed [12] that in the stress corrosion process the oxide layers *in statu nascendi* are of importance we wished to gain information on the newly formed oxide layers as well, especially on the influence of the magnesium content of the alloy on the oxide layer. This problem was investigated by the use of secondary-ion mass-spectrometry (SIMS).

The oxide layers were prepared *in situ* in the investigating device itself. First the oxide was removed in ultra-high vacuum from the surface to be studied by ion bombardment. The ion dose needed for this purpose was about 0.05 C cm⁻², therefore the surface of the sample was rather rough after this treatment. Fig. 1 shows the morphology of an ion bombarded surface.

Afterwards the initial oxide layers were permitted to form and their ionic spectra were investigated.

The oxide layers were formed by exposing the surface to different oxygen pressures for different time intervals. At the start of the measurements we also obtained the ionic spectra of the natural oxide layers; these data are also reported here.

The SIMS investigations were carried out using Balzers equipment. The background pressure was 10⁻⁹ Torr, the pressure of Ar gas was 10⁻⁸ to

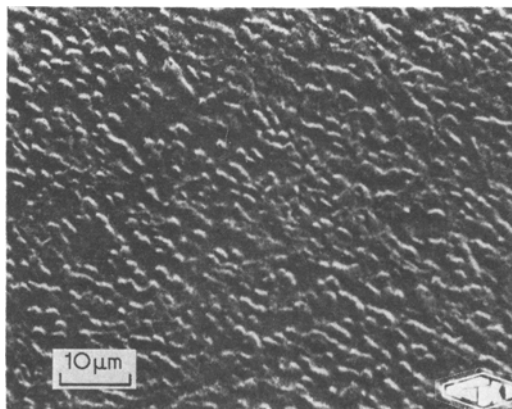


Figure 1 Scanning electron micrograph of an ion-bombarded surface.

10⁻⁵ Torr during sputtering. The oxygen pressure could be varied corresponding to the different oxygen doses in a range of 10 H to 4 × 10⁴ L. (L = Langmuir = 10⁻⁶ Torr sec). After the proper oxygen dose had been given, we started the SIMS investigation. The Ar⁺ ion beam of current density 2 × 10⁻⁶ A cm⁻² and 3 keV energy sputtered the sample at an angle of 30°. Further details of the measurement are given elsewhere [13, 14].

Table I gives the compositions of the alloys. All alloys were prepared from high-purity materials, with the exception of the commercial alloy Al–3.2% Zn–2.4% (No. 4).

Fig. 2 shows a SIMS spectrum. Since sputtering was carried out with argon ions we used the negative spectrum for detecting magnesium oxide.

To permit a better survey, we have summarized in Table II the secondary ion intensity ²⁴Mg⁺ and ⁴⁰MgO⁻ values – obtained by argon sputtering – of the oxide layers formed in the atmosphere and made *in situ* on the alloys Table I.

From our investigations we conclude that the aluminium oxide layer formed on the surface of Al–Mg and Al–Zn–Mg alloys is not a pure amorphous Al₂O₃ layer but also contains MgO. Taking into account the values of the free enthalpy of formation the amount of MgO as compared with the Mg content is relatively low. However, according to our investigations a higher

TABLE I

No. of sample	Mg (wt %)	Zn (wt %)
1	1.1	–
2	2.4	–
3	4.6	–
4	2.4	3.2

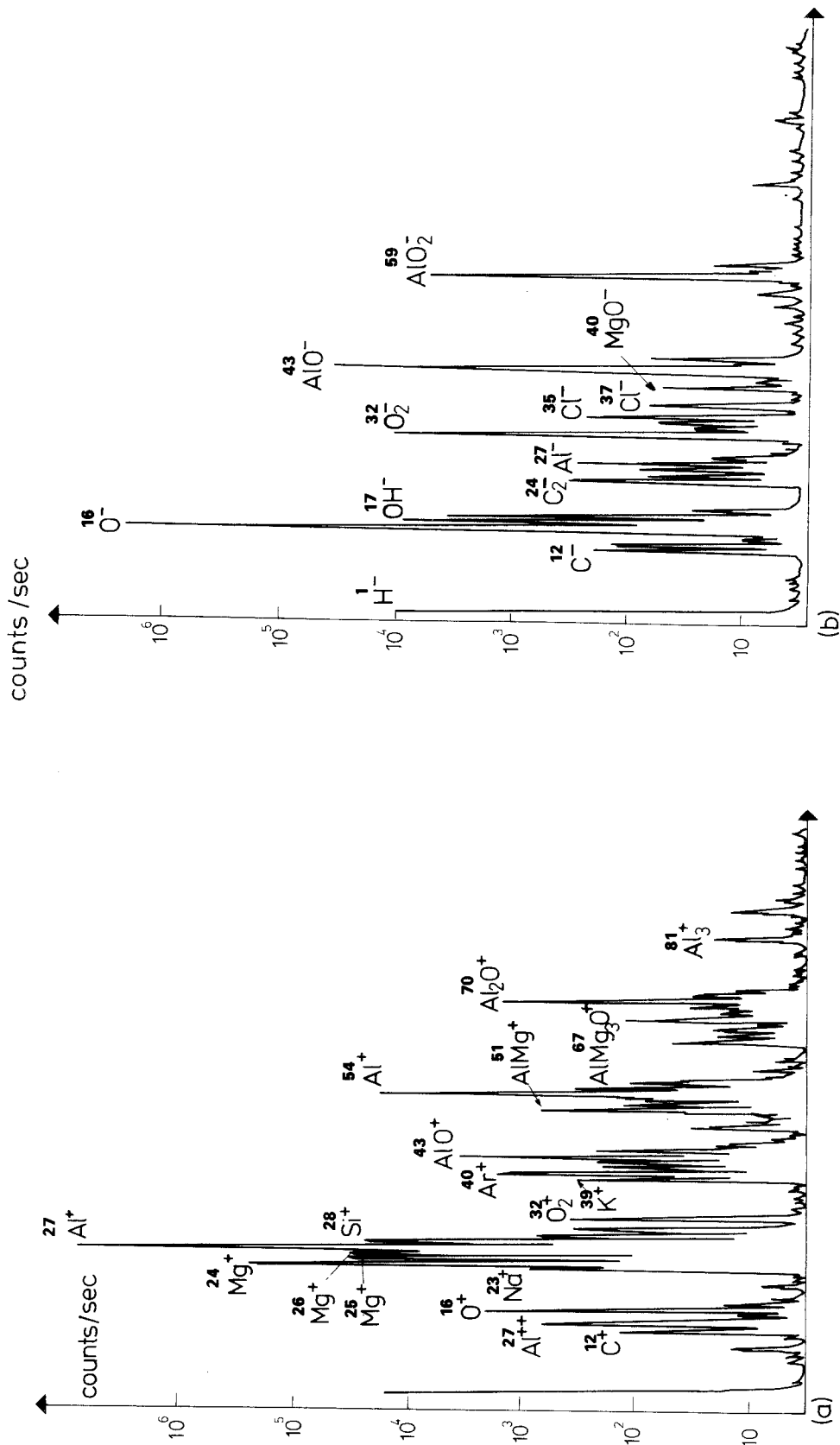


Figure 2 (a) positive and (b) negative spectrum of the oxide layer obtained at the surface of an Al-2.4% Mg alloy, with an oxygen dose of 4×10^4 L, sputtered with argon ions in a vacuum of 1.33×10^{-7} Pa.

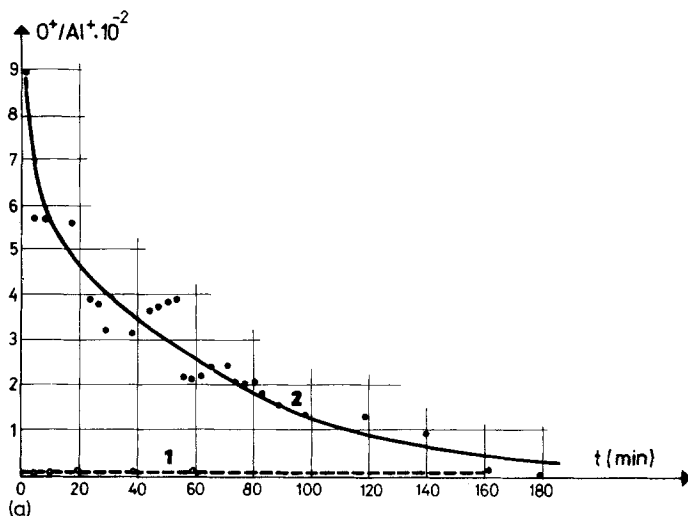
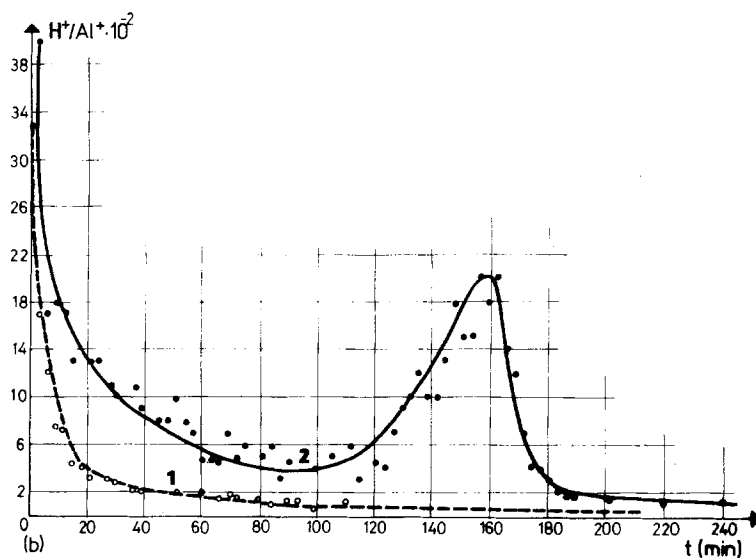


Figure 3 Depth profile of the surface of an Al-4.7% Zn-1.7% Mg alloy, coated with a natural oxide layer (1) and a thermal oxide layer (2), afterwards stored for 10 days at 50° C in 100% r.h. (a) from $O^+/Al^+ \times 10^{-2}$ SIMS spectra (b) from $H^+/Al^+ \times 10^{-2}$ SIMS spectra.



Mg content results in a higher MgO content in the amorphous oxide layer, i.e. in a layer which is more permeable than pure aluminium oxide to the entry of hydrogen or water vapour and promotes stress corrosion cracking.

2.2. The effect of the thermal oxide layers

As we know, the so-called pre-exposure embrittlement of Al-Zn-Mg alloys can be increased substantially when a thermal oxide layer is formed on their surface [1, 16]. Scamans *et al.* have used *in situ* hydrogen measurements made directly during the rupturing of the samples to detect with a mass spectrometer the hydrogen evolved from the samples during rupture. We have repeated their pre-corrosion experiment and obtained SIMS spectra of the pre-corroded samples to study the

position of the hydrogen relative to the oxide layer and the changes of microstructure in the course of these investigations with the aid of other electrom beam methods.

Fig. 3a shows the SIMS profiles of a natural oxide layer [1] and a pre-corroded sample covered with a thermal oxide layer [2], plotted from the secondary ion intensity O^+ SIMS values.

Fig. 3b shows the H^+ profiles for the above samples and for the oxide layers on their surfaces.

The different ion profiles were obtained quasi simultaneously by an automatic control system which switched the quadrupole supply from one mass number to another in every second. Hydrogen determination was carried out with the equipment and method described in literature [15].

The comparison of Figs. 3a and b clearly shows

TABLE II

No. of sample	Dosage	Sputtering current (I_m)	Secondary ion intensity $^{24}\text{Mg}^+$	Secondary ion intensity $^{40}\text{MgO}^-$
1	atmosphere	1×10^{-7}	7.0×10^4	1.8×10
	$4 \times 10^4 \text{ L}^*$	5×10^{-7}	7.0×10^7	1.1×10
2	atmosphere	1×10^{-7}	1.4×10^5	8.0×10
	$4 \times 10^4 \text{ L}$	5×10^{-7}	2.2×10^5	5.0×10
3	atmosphere	1×10^{-7}	2.5×10^5	2.4×10^2
	$4 \times 10^4 \text{ L}$	5×10^{-7}	8.0×10^5	3.0×10^2
4	atmosphere	1×10^{-7}	5.0×10^4	2.5×10
	$4 \times 10^4 \text{ L}$	5×10^{-7}	2.0×10^5	4.3×10

*L = Langmuir = 10^{-6} Torr sec.

that in the sample with the thermal oxide layer, there is a strong maximum of hydrogen located between the oxide layer and the metal.

The samples of 0.5 mm thickness, studied with the SIMS method, were ruptured on the tensile testing machine. Fig. 4 shows the difference in fracture surfaces on scanning electron micrographs. The sample coated with a thermal oxide layer is clearly embrittled. Fig. 5 shows the structure of the thermal oxide layer obtained by heat treatment observed in a transmission electron microscope. During the formation *in situ* of crystalline oxide phases the priority and importance of grain boundaries is very evident. The crystalline oxides increase the water vapour permeability of the oxide mainly at the grain boundaries.

As shown by our measurements with an electron beam microanalyser [17] a zone poor in oxide forming agent (Mg) has appeared in parallel with oxide formation. The dimensions of this zone

are shown in Fig. 6. A difference in structure of this zone as compared with the bulk material can also increase precorrosion sensitivity. The concentration of the alloying element was measured from point to point along the diameter of the freshly cut surfaces. The diameter of the electron-beam was $1 \mu\text{m}$.

3. Conclusions

From literature data and the results of our own measurements the following model for the stress corrosion mechanism in Al-Zn-Mg alloys can be sketched:

The PFZ composition is different from that of the interior of the grain in a twofold sense: it has a higher Mg content and a lower equivalent Zn content. In the PFZ the dislocation movement is increased under the influence of mechanical stresses, probably because of the reduction in Zn content. The relatively increased Mg content in the

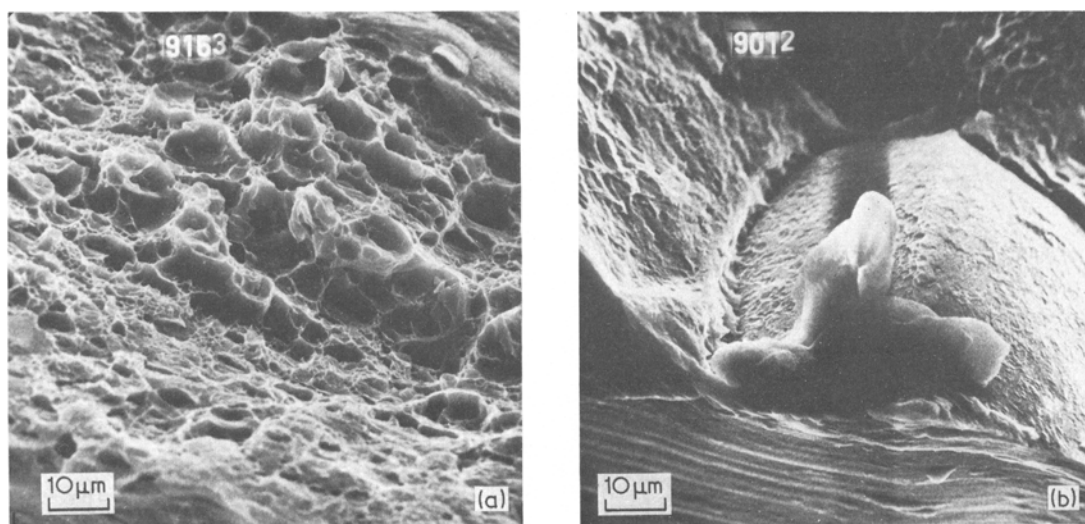


Figure 4 Fracture surfaces of the samples which furnished the surface profiles shown in Fig. 3, (a) sample coated with a natural oxide layer, (b) sample coated with a thermal oxide layer. Scanning electron micrographs.

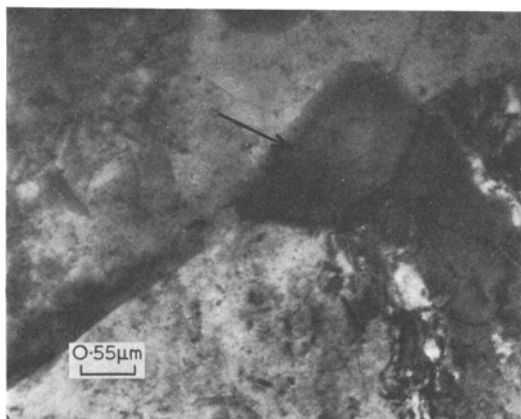


Figure 5 MgO crystals formed on the surface of an Al-3.2% Zn-2.4% Mg alloy at 450°C. Transmission electron micrograph.

grain boundary region results in an oxide layer with increased MgO content which is less effective as a barrier against environmental influences. Further this compositional and structural inhomogeneity of the oxide layer explains its decreased resistance to mechanical stresses and results in increased slip in the zone carrying the layer. This is in accordance with the experience of Tuck and Scamans [11] that the penetration of water vapour through the amorphous oxide layer of Al-Zn-Mg alloys sensitive to stress corrosion occurs primarily in the PFZ.

This effect can be strengthened by establishing a thermal oxide layer on the alloy surface; then the alloying element content of the substrate metal layer near the surface is reduced and crystalline oxides which form primarily at the grain boundaries further facilitate the penetration of water vapour in the metal.

During the water vapour-metal reaction, occurring immediately below the oxide layer, hydrogen is distributed in the sample, partly between the oxide layer and the metal (see Fig. 3) and partly along the grain boundaries (see Fig. 4), leading to intercrystalline fracture. It is well known that fracture surfaces of samples subjected to stress corrosion are also of an intercrystalline type [8]. The assumption of a partially similar mechanism for these two fractures seems justified but requires further proof.

Acknowledgements

The authors wish to thank Dr V. Stefányai for the electron beam microanalyser measurements and to Dr G. Groma for valuable discussions.

References

1. L. MONTGRAIN and P. M. SWANN, "Hydrogen in Metals", edited by J. M. Bernstein and A. W. Thompson, (ASM, Metals Part, Ohio, 1974) p. 575.
2. R. J. GEST and A. R. TROIANO, *Corrosion* 30 (1974) 274.
3. L. KNUTSSON, *Corrosion* 12 (1977) 447.
4. K. G. KENT, *Australian Inst. Metals J.* 15 (1971) 171.
5. D. E. WARD and G. W. LORIMER, Proceedings of the Third International Conference on the strength of Metals and Alloys, Cambridge, (1973) Vol. 1, p. 488.
6. P. DOIG, J. W. EDINGTON and G. HIBBERT, *Phil. Mag.* 28 (1973) 971.
7. K. G. KENT, *J. Inst. Metals* 97 (1969) 127.
8. D. A. VERMILYEA, "Fundamental aspects of stress corrosion cracking", Proc. Conf. 1967, Ohio State University, National Association of Corrosion Engineers, Houston, (1969) p. 15.
9. K. BANIZS and L. VITALIS, *Z. Metallk.* 68 (1977) 554.

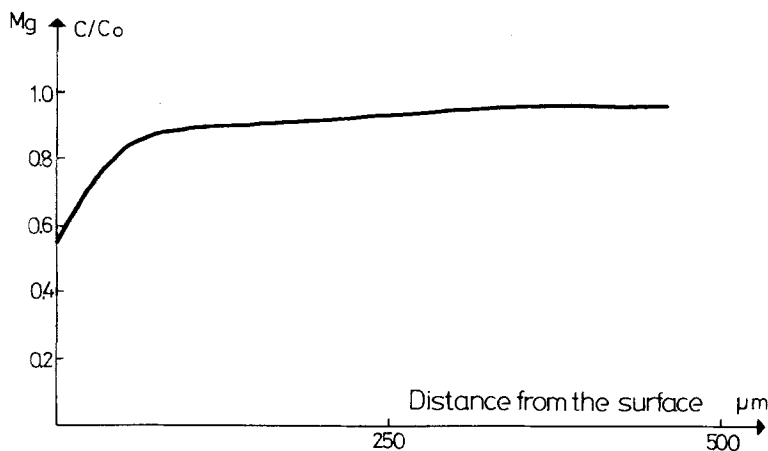


Figure 6 Alloying element depletion in the vicinity of the surface of an Al-3.5% Zn-1.2% Mg alloy after 6 hours at 500°C.

10. D. O. SPROWLS and R. H. BROWN, "Fundamental aspects of stress corrosion cracking", Proc. Conf. 1967, Ohio State University, National Association of Corrosion Engineers, Houston, (1969) p. 466.
11. C. D. S. TUCK and G. M. SCAMANS, "Hydrogen in Metals", Proceedings of the 2nd International Congress, Paris, France (1977) p. 411.
12. D. A. VERMILYEA, General Electric Report No. 71 c-228, 1971, (Schenectady, New York, General Electric Company).
13. J. GIBER, *Thin Solid Films* **32** (1976) 295.
14. D. MARTON and Á. CSANÁDY, *Nederlands tidschrift voor vacuum-techniek* **16** (1978) 47.
15. F. PAVLYAK, L. BORI, J. GIBER and R. BUHL, *Japan. J. Appl. Phys.* **16** (1977) 335.
16. G. M. SCAMANS, R. ALANI and P. R. SWANN, *Corros. Sci.* **16** (1976) 443.
17. Á. CSANÁDY, V. STEFÁNIAY and D. BEKE, accepted in *J. Mater. Sci. Eng.*
18. Á. CSANÁDY and L. VITÁLIS, *Aluminium (Düsseldorf)* **54** (1978) 452.

Received 3 November 1978 and accepted 28 February 1979.